Characterization of the mouse metal-regulatory-element-binding proteins, metal element protein-1 and metal regulatory transcription factor-1

Olivier LAROCHELLE*†, Gale STEWART*†, Pierre MOFFATT*†, Véronique TREMBLAY*† and Carl SÉGUIN*†[1]

*Centre de recherche en cancérologie de l'Université Laval, CHUQ, Hôtel-Dieu de Québec, 11, côte du Palais, Québec, QC, Canada G1R 2J6, and †Département d'anatomie et de physiologie, Faculté de médecine, Université Laval, Québec, QC, Canada G1K 7P4

Metal activation of metallothionein gene transcription depends mainly on the presence of regulatory DNA sequences termed metal-regulatory elements (MREs) and involves MRE-binding transcription factor-1 (MTF-1) interacting with the MREs in a Zn^{2+}-dependent manner. We previously identified and characterized a nuclear protein, termed metal element protein-1 (MEP-1), specifically binding with high affinity to MRE elements. The precise relationship between MTF-1 and MEP-1 was unclear, and to determine whether MEP-1 and MTF-1 were distinct protein species, we performed DNA binding analyses to characterize the binding properties of both proteins. Electrophoretic mobility-shift assays showed that MTF-1, produced in COS cells, produces a slower-migrating band compared with that obtained with purified MEP-1. Using an anti-MTF-1 antibody, we showed that both the MTF-1–MRE and the MEP-1–MRE complexes are supershifted by an anti-MTF-1 antibody, thus demonstrating that MEP-1 is antigenically related to MTF-1. RNase protection analyses carried out with RNA prepared from different tissues and cell lines failed to reveal the presence of MTF-1 splicing variants. This indicates that MEP-1 may be a proteolytic fragment of MTF-1. MTF-1 DNA-binding activity was rapidly activated *in vivo* by Zn^{2+} ions but not by Cd^{2+}, UV irradiation or PMA, and occurred on ice as well as at 21 °C. In control and Zn^{2+}-treated cell extracts, DNA-binding activity was not enhanced *in vitro* following the addition of exogenous Zn^{2+} or a preincubation at 37 °C. However, recombinant MTF-1 produced *in vitro* required Zn^{2+} activation for DNA binding. Interestingly, treatment of nuclear extracts with calf intestine phosphatase completely abrogated MTF-1 DNA-binding activity, thus suggesting that phosphorylation is involved in the regulation of MTF-1 activity.

Key words: inducible gene expression, metalloregulatory transcription factors, metallothionein gene, phosphorylation, splicing.

INTRODUCTION

Metallothioneins (MTs) are small cysteine-rich, metal-binding stress proteins that play important roles in Zn^{2+} and Cu^{+} homoeostasis and in detoxification of toxic metals [1,2]. MT genes are universally inducible at the transcriptional level by a variety of stress conditions that include metals, hormones, cytokines, xenobiotics, hypoxia, reactive oxygen species (ROS), and UV irradiation. The MT genes represent well-understood examples of metal-regulated genes, and provide an excellent model system for understanding how expression of a eukaryotic gene is modulated in response to metals, and for characterizing the signal-transduction pathway involved in this modulation. Metal activation of MT gene transcription is dependent on the presence of metal regulatory elements (MREs), which are present in five non-identical copies (MREa–MREe) in the 5′ flanking region of the mouse MT-1 gene [3,4], and on the capacity of MRE-binding transcription factor-1 (MTF-1) to bind to the MREs in the presence of Zn^{2+} and induce transcription [5,6].

MTF-1 is a 72.5 kDa Zn-finger protein that contains a unique N-terminal domain and a DNA-binding domain of six Zn-fingers of the TFIIIA type (C_2H_2), followed by three distinct activation domains which are characterized by a high density of acidic residues, proline residues, and serine/threonine residues respectively [5,7]. MTF-1 gene knock-out by homologous recombination in mouse ES cells showed that MTF-1 is essential for basal and metal-induced transcription [6]. A role of MTF-1 in the activation of MT gene transcription in response to ROS [8] and hypoxia [9] has also been reported, indicating that MTF-1 is a multistress-responsive factor. The recent characterization of MTF-1 from the Japanese pufferfish (*Fugu rubripes*) revealed a structural and functional conservation of this protein over 400 million years of evolution, supporting the notion that MTF-1 is an important eukaryotic stress sensor [10].

No MRE-binding protein could be detected in MTF-1-null mutant ES cells [6]. This led to the hypothesis that MTF-1 is the only factor that binds MREs and the only transcription factor that mediates responsiveness to different metals [6,11]. However, a number of MRE-binding proteins have been detected *in vitro* by different DNA binding assays, including MEP-1, ZRF, M96/ZiRF1, ZAP, MREBP, MREBP-34, MafY, p39, MRE-BF1 and MRE-BF2 [12]. Amino acid sequences obtained from ZRF tryptic peptides revealed that ZRF corresponds to human MTF-1 [13], whereas co-transfection experiments suggest that ZiRF1 (zinc-regulated factor-1) may be involved in regulation of MT gene transcription by metal ions [14]. However, the functional

Abbreviations used: CIP, calf intestine phosphatase; EMSA, electrophoretic mobility-shift assay; FCS, fetal-calf serum; MEP-1, metal element protein-1; MRE, metal-regulatory element; MRE-s, a synthetic MRE consensus sequence; MT, metallothionein; MTF-1, MRE-binding transcription factor-1; oligo, oligonucleotide; pKS, pBlueScript/KS; ROS, reactive oxygen species; RT-PCR, reverse-transcription PCR; PKC, protein kinase C; NF, nuclear factor.

[1] To whom correspondence should be addressed (e-mail Carl.Seguin@crhdq.ulaval.ca).

relevance of the other proteins to MT gene transcription has not yet been demonstrated.

We previously identified and characterized a mouse nuclear protein, termed metal element protein-1 (MEP-1), specifically binding with high affinity to MRE elements in a Zn^{2+}-dependent manner [15,16]. The nucleotide sequence recognized by MEP-1 is the same as that required for *in vivo* transcriptional activity of mouse MREd and that required for the binding of MTF-1 [16]. In addition, both MEP-1 [16] and MTF-1 [5] migrate on a denaturing gel with an M_r of approx. 100000, as assayed by Southwestern analysis. The precise relationship between MTF-1 and MEP-1 is still unclear, and to determine whether MEP-1 and MTF-1 were distinct protein species, DNA-binding analyses were performed using purified MEP-1 and MTF-1 produced in COS cells. RNase protection analysis was also carried out with RNA prepared from different tissues and cell lines to identify putative MTF-1 splicing variants.

EXPERIMENTAL

Cell culture, treatments and nuclear-extract preparations

For large-scale nuclear-extract preparations, heavy-metal-resistant mouse L50 cells (obtained from Dr Dean H. Hamer, Laboratory of Biochemistry, Division of Basic Sciences, National Cancer Institute, National Institutes of Health, Bethesda, MD, U.S.A.) were grown in suspension in Eagle's minimum essential medium (Spinner modification; Sigma catalogue number M4767; 'SMEM') supplemented with 5% (v/v) fetal-calf serum (FCS) and 5% (v/v) horse serum in the continuous presence of 15 μM $CdCl_2$ and 5 μM $ZnCl_2$ by Cellex Biosciences, Inc. (Minneapolis, MN, U.S.A.). For small-scale analytical experiments, L50, as well as L, NIH-3T3, COS-7, dko7 ([7]; generously donated by Dr Walter Schaffner, Institut für Molekularbiologie, University of Zurich, Zurich, Switzerland), TM3 and TM4 cells were cultured in monolayer in Dulbecco's modified Eagle's medium supplemented with 10% FCS. Mouse P19 EC cells were maintained in α-minimum essential medium containing 7.5% calf serum and 2.5% FCS as described in [17]. For heavy-metal induction, cells were incubated in the presence of $CdCl_2$ (final concn. 2.5 μM) or $ZnSO_4$ (100 μM), for 30 min–8 h before harvesting, as indicated in the Figure legends. For UVC irradiation, exponentially growing cells were washed twice with PBS, irradiated with a UV germicidal lamp (λ_{max} 254 nm, 100 J/m^2) and cultured in the original culture medium for 8 h. PMA (100 ng/ml; Sigma, St Louis, MO, U.S.A.) was added to the culture media 1–8 h before harvesting. To obtain MTF-1-enriched nuclear extracts, COS-7 cells were transfected by calcium phosphate precipitation [18] with 10 μg of the eukaryotic expression vector pC-mMTF-1a [5] (kindly provided by Dr Walter Schaffner) or pCDNA3-MTF-1, and treated or not for 30 min with $ZnSO_4$ (100 μM). To prepare the expression vector pCDNA3-MTF1, a mouse MTF-1 *Ava*I fragment was first excised from pC-mMTF-1a and cloned in the *Ava*I site of pBluescript/KS (pKS) vector (Stratagene, La Jolla, CA, U.S.A.) to generate pKS-MTF-1. The 5′ end of the MTF-1 *Ava*I insert contains 14 bp of vector sequences and the 3′ end 306 bp. Then MTF-1 was excised from pKS-MTF-1 as a *Xho*I–*Not*I fragment and cloned into the *Xho*I–*Not*I sites of plasmid pCDNA-3 (Invitrogen, Carlsbad, CA, U.S.A.). To prepare the deletion mutants of MTF-1, the plasmid pKS-MTF-1 was digested with *Apa*I, *Eco*RI, or *Nar*I and *Cla*I and re-circularized with T4 DNA ligase to create pKS-MTF1/*Apa*I, pKS-MTF1/*Nar*I and pKS-MTF1/*Eco*RI. MTF-1 sequences were then excised as *Xho*I–*Not*I fragments from the respective pKS-based vectors and cloned into the *Xho*I–*Not*I sites of vector pCDNA-3.

Large L50-cell nuclear extracts were prepared as described in [19], except that the final dialysis step was omitted and that all buffers contained 10 μM $ZnCl_2$. Preparation of small-scale nuclear extracts was performed as described by Schreiber et al. [20] with minor modifications, namely the omission of Zn^{2+}, EDTA and EGTA from the buffers in order to insure minimal interference in the basal metal equilibrium and obtain extracts as much as possible representative of the conditions *in vivo*.

Chromatography, DNA-binding analyses and partial proteolytic digestion

MEP-1 was purified by standard chromatography with NaCl gradient elution [16]. Briefly, 60 ml of L50-cell crude nuclear extracts (10 μg of total proteins/μl) were applied on to a 60 ml heparin–Sepharose CL 6B (Amersham Pharmacia Biotech, Baie d'Urfé, QC, Canada) column and eluted with a NaCl gradient (325–1500 mM). Fractions containing the DNA-binding activity were pooled, diluted to a final concentration of 130 mM NaCl and loaded on to a 1 ml DNA-affinity column containing the concatenated oligonucleotide (oligo) mouse MREa [16]. The bound proteins were eluted with a NaCl gradient (130–1000 mM). The active fractions were pooled, diluted to 130 mM NaCl and rechromatographed on the same affinity column, resulting in purified MEP-1. Throughout purification, all buffers were supplemented with 50 μM $ZnCl_2$. BSA (250 μg/ml; Life Technologies, Burlington, ON, Canada) was also added to the elution buffers for the heparin–Sepharose column and the first round of affinity chromatography.

For the electrophoretic mobility-shift assay (EMSA), double-stranded MRE-s, a synthetic MRE consensus sequence [5], or mMT1-Sp1A (5′-gatcCCAAAGGGGCGGTCCCGCTa-3′, provided with *Bgl*II sites) was synthesized and end-labelled with [γ-^{32}P]ATP (NEN, Boston, MA, U.S.A.) (5000–10000 c.p.m./fmol). The Sp1 oligo corresponds to the sequence of the Sp1-A site (nucleotides −192 to −173, relative to the transcription start point) in the promoter of the mouse MT-1 gene. Binding reaction mixtures contained, in a final volume of 12 μl, 2 μg of COS-MTF-1 nuclear extract or 1 μl (approx. 2 ng) of purified MEP-1, 20 fmol of labelled DNA, 500 ng of poly(dI-dC) (Amersham Pharmacia Biotech), 15 mM Hepes, pH 7.9, 2 mM $MgCl_2$, 50 mM NaCl, 0.8 mM dithiothreitol, 0.4% Nonidet P40 and 3.3% Ficoll. Reaction mixtures were incubated for 10 min on ice or at 21 °C, as indicated in the Figure legends, before loading on a 6%-polyacrylamide gel [acrylamide/bisacrylamide, 29:1 (w/w)] in 0.5% Tris/borate buffer and electrophoresed at 10 V/cm at 21 °C. After electrophoresis, the gel was dried, and labelled complexes were detected by autoradiography. For competition experiments, 2 pmol of the unlabelled, double-stranded, MRE-s oligos, mouse MREa [15], or the non-functional MRE mutant, MUTds [21], were added together with the probe. Variations from these assay conditions are as described in the Figure legends and Results section. Effects of incubation temperature and time were examined. Binding reaction mixtures were preincubated at 37 °C for 15 min, the probe was added, the mixtures incubated on ice or at 21 °C for another 10 min, and protein–DNA complexes were separated by PAGE. Effects of the addition of exogenous metals or EDTA on MEP-1–MRE and MTF-1–MRE-s complex-formation were also examined. EMSA reaction mixtures containing labelled MRE-s oligo, purified MEP-1 or MTF-1-enriched COS-cell extracts were sequentially incubated for 10 min at 21 °C with 100 μM EDTA, 10 min on ice or at 21 °C in the presence of 0, 5, or 50 μM of different cations, and 10 min on ice with the MRE-s probe before PAGE. Signal intensities of protein–DNA com-

plexes were quantified using a PhosphoImager 860 and ImageQuant 4.2 software (Molecular Dynamics).

In proteolytic EMSA, binding reaction mixtures containing MTF-1-enriched COS-cell nuclear extracts or purified MEP-1 were incubated in the presence of various concentrations of thrombin (Roche Diagnostics, Laval, QC, Canada) or staphylococcal proteinase V8 (Sigma) for 2–30 min at 21 °C. Then the labelled MRE-s probe was added to the reaction mixtures, binding was allowed to proceed for 10 min on ice, and samples were analysed by PAGE.

In antibody competition EMSA experiments (supershift assays), 1 μl of an anti-MTF-1 (generously provided by Dr Walter Schaffner) or an anti-MT-3 (P. Moffatt and C. Séguin, unpublished work) polyclonal antibody was added to the binding reaction mixture, which was incubated for 5 min on ice or at 21 °C, followed by addition of the labelled MRE-s probe.

To determine whether MTF-1 DNA binding is phosphorylation-dependent, L50- or MTF-1-enriched COS-cell nuclear extracts (2 μg) or purified MEP-1 (1 μl) were incubated with 1 unit of calf intestine phosphatase (CIP; Roche Diagnostics) for 5 or 15 min at 21 °C. As a control, CIP was boiled for 15 min before incubation with extracts. Phosphatase reactions were stopped with 1 mM sodium vanadate and NaF and 50 mM β-glycerophosphate. The phosphatase-treated samples were incubated for 10 min on ice with ^{32}P-labelled MRE-s oligos and separated by PAGE as described above.

DNaseI footprinting assays were performed [16] using a mouse MT-1 PCR-amplified fragment, position -348 to $+72$, as the probe. For the PCR reaction, the oligos mMT1.Bst (5′-GTTACCACGCTGCGAATGG-3′), ^{32}P-labelled in 5′ with polynucleotide kinase, and mMT1.72 (5′-CCGAGATCTGGTGAAGCTGGAGCTACGGAG-3′) were used. Footprinting competition experiments were performed as described above, using as competitors the double-stranded oligo mouse MREd. Western analysis was performed using the anti-MTF-1 polyclonal antibody (1:2000) and the Immune Select™ alkaline phosphatase NBT/BCIP (Nitroblue Tetrazolium/5-bromo-4-chloroindol-3-yl phosphate) detection kit (Life Technologies) according to the manufacturer's instructions.

Recombinant MTF-1 was synthesized *in vitro* by using the TnT-coupled reticulocyte-lysate system (Promega, Madison, WI, U.S.A.), 250 ng of the plasmid pKS-MTF-1 and T7 RNA polymerase, as suggested by the manufacturer.

RNase protection analyses

Total RNA from different tissues was extracted with guanidium isothiocyanate and purified through a CsCl cushion ultracentrifugation step [22], whereas that from cultured cells was extracted with guanidium isothiocyanate [18]. Vectors for preparing radiolabelled antisense MTF-1 riboprobes for RNase protection were constructed as followed: For pMTF1-S1 and pMTF1-S2 (to generate probe *S-1* and *S-2*, Figure 4B below), plasmids pKS-MTF1/*Eco*RI and pKS-MTF1/*Nar*I were digested with *Pst*I and *Bam*HI or *Eco*RI and *Bam*HI, respectively, rendered blunt with Klenow DNA polymerase and recircularized with T4 DNA ligase; to construct the pMTF1-S3 vector (probe *S-3*), a *Pst*I–*Pst*I fragment (nucleotides 1364–1781) was excised from pKS-MTF-1 and subcloned into the *Pst*I sites of pKS; to create pMTF1-S4 (probe *S-4*), DNA fragments (nucleotides 800–1128) from mouse MTF-1 cDNA were generated by PCR amplification, using the oligos MTF1-800, 5′-cgacgcggccGCAGCAAATACTTCACCAC-3′ (*Xho*I site underlined), and MTF1-1128, 5′-gcggctcgaGGACAGAAGGCCCAGCTC-3′ (*Not*I site underlined), and subcloned into the *Not*I–*Xho*I sites of pKS. For all the constructs the identity of the fragments was confirmed by sequencing.

The plasmids were then linearized by using the *Not*I or *Eco*RI (probe *S-3*) restriction site. Antisense riboprobes were synthesized using T3 (probe *S-1*, *S-2*, and *S-4*) or T7 (probe *S-3*) polymerase (MBI Fermentas, Flamborough, ON, Canada), depending on the orientation of the insert, in the presence of [^{32}P]CTP (800 Ci/mmol; Amersham Pharmacia Biotech). These probes also contained, at their 5′ end, sequences of pKS corresponding to DNA between the T7 or T3 promoter and the restriction sites where the DNA fragments were inserted and, at their 3′ end, to sequences between the cloning restriction site and the *Not*I (or *Eco*RI) site used to linearize the plasmids. This extra DNA had a total size of 103 bp for probe *S-1*. Full-length, radiolabelled cRNA was purified by two succesive ethanol precipitations. The labelling efficiency was determined by liquid-scintillation counting, and approx. 5×10^5 c.p.m. of each labelled riboprobe were used per reaction. The RNA protection assay was performed essentially as described in [23,24]. Briefly, the labelled riboprobes were annealed to 20 μg of total RNA in formamide buffer. Hybridization was done for 12 h at 60 °C. Following annealing, unprotected single-stranded RNA was digested with a mixture of RNase A (Roche Diagnostics; 6.25 μg/ml) plus RNase T1 (Roche Diagnostics; 250 units/ml). Double-stranded RNA fragments were sized on 6% denaturing polyacrylamide gels. As a negative control each riboprobe was annealed to yeast tRNA (Sigma) and incubated with the RNase mixture. After electrophoresis, the gel was vacuum-dried and exposed to X-ray film overnight with an intensifying screen at -80 °C.

Reverse-transcription (RT)-PCR and DNA sequencing

For the RT-PCR assay, 5 μg of NIH-3T3 cell total RNA was mixed with 10 μM of oligo(dT)$_{12-18}$ (Amersham Pharmacia Biotech) or the MTF1-1167 (5′-ccggatccGGTCCTGTGTCGAACTGG-3′, *Bam*HI site underlined) oligo and 200 units of Superscript II RNase H$^-$ reverse transcriptase (Life Technologies) in a final volume of 20 μl. The reverse transcription was performed for 50 min at 42 °C according to the manufacturer's instructions. For PCR, 2 μl of the first-strand reaction was mixed with oligo primers MTF1-845 (5′-ccggatccATACAGGAGAAAAGCCATTTCG-3′, *Bam*HI site underlined) and MTF1-1128, and PCR reactions were performed for 30 cycles in a thermal cycler (Perkin–Elmer Cetus, Montréal, QC, Canada). The PCR fragment was isolated using the extraction kit QIAquick (Qiagen, Mississauga, ON, Canada), and cloned into the *Bam*HI site of pKS. *Escherichia coli* DH5α cells were transformed with the resulting plasmids and six different clones were sequenced by means of vector-derived primers (Stratagene). Sequencing reactions were carried out by the dideoxy-chain-termination method [25] on mini-scale preparations of subcloned DNA precipitated by cetyltrimethylammonium bromide [26], using a T7 DNA polymerase sequencing kit (Amersham Pharmacia Biotech). Nucleic acid sequences were analysed with software from the Wisconsin Package Version 10 [University of Wisconsin Genetics Computer Group (GCG), Madison, WI, U.S.A.].

RESULTS

Purification and characterization of MEP-1

MEP-1 was purified from 60 l of L50 cells using a combination of heparin–Sepharose and MRE-affinity chromatography. The purification of MEP-1 was monitored using SDS/PAGE, DNaseI

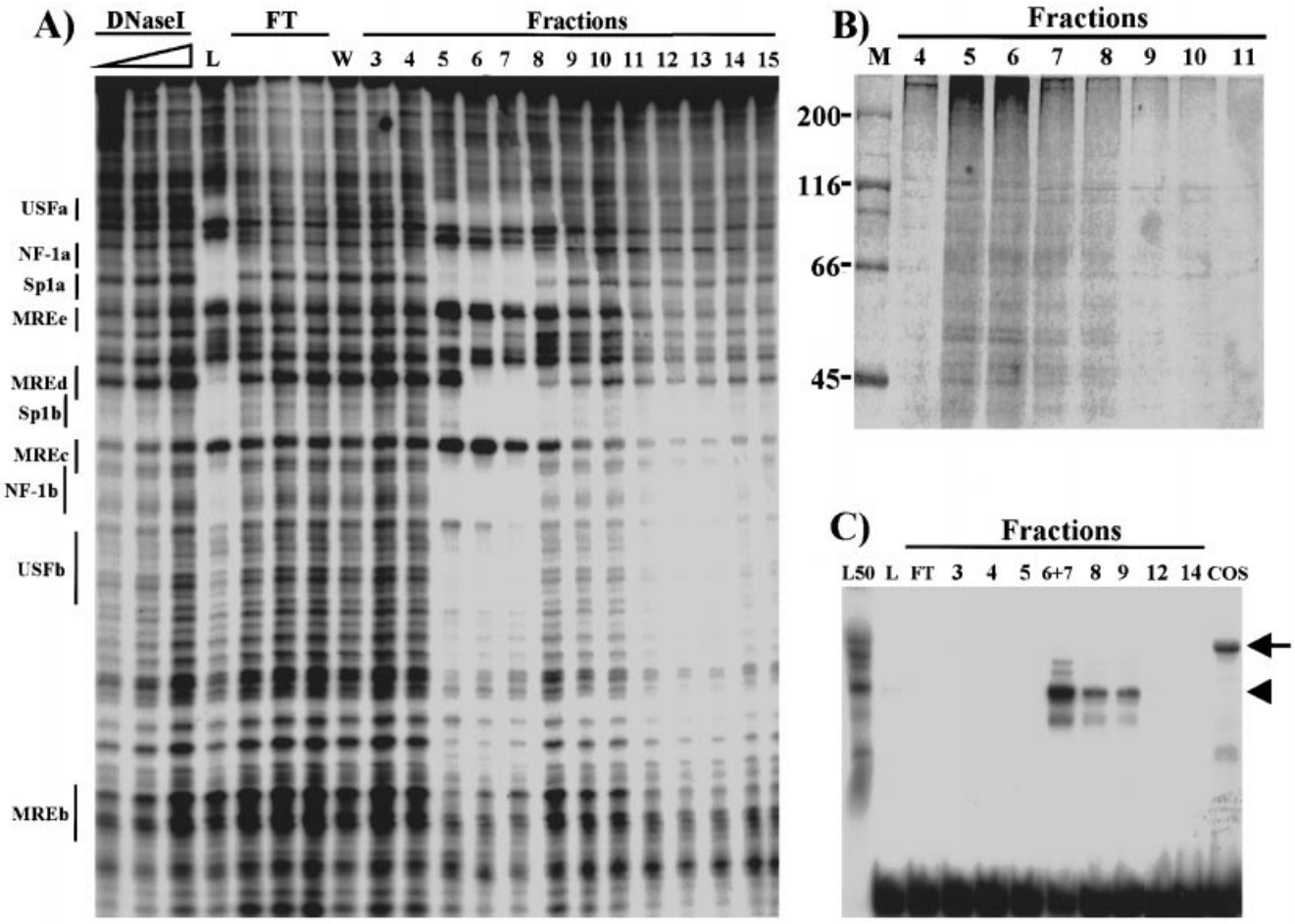

Figure 1 Purification of MEP-1

(**A**) DNaseI footprinting analysis of chromatographic fractions. Aliquots (15 μl) of the second-affinity-column fractions (3–15) were added to the different reaction mixtures as indicated. The probe was a mouse MT-1 gene promoter DNA fragment extending from positions -348 to $+72$. The amount of DNaseI varied from 0.5 to 2 μg on bare DNA template as indicated schematically over the lanes. Lanes: L, load; FT, flow through; W, wash. The positions of the different *cis*-acting elements are indicated on the left as determined by Maxam–Gilbert sequencing. (**B**) Protein profile of MEP-1 purification; 20 μl of second-affinity-column fractions as indicated were analysed on an SDS/8%-polyacrylamide gel, followed by Silver staining. Numbers (in kDa) on the left refer to molecular-mass markers (M). (**C**) EMSA. Reactions were carried out by incubating a ^{32}P-labelled synthetic oligo, MRE-s (20 fmol), with 2 μg of nuclear extracts prepared from L50 cells (L50) or COS cells transfected with a mouse MTF-1 expression vector (COS), or 1 μl of the second-affinity-column fractions shown in (**A**), as indicated. Arrow, the MTF-1–DNA complex; arrowhead, the MEP-1–DNA complex. Lane L, load. Autoradiograms were digitally generated using a Hewlett–Packard Scan Jet 6100C/T and Desk Scan II 2.3 software.

footprinting, EMSA and Western analyses. DNaseI footprinting reactions, performed with the different chromatographic fractions of the second MRE-affinity column, showed that MEP-1 was mainly eluted in fractions 6 and 7 (Figure 1A). MEP-1 is defined here as the MREd-binding activity, since the protection present at the nuclear factor-1b (NF-1b) site around the MREc element involves an NF-1-like protein that also binds to the upstream NF-1a site (O. LaRochelle, V. Tremblay, S. Labbé and C. Séguin, unpublished work), and that at the upstream stimulatory factor b (USFb) site appears to be generated by the transcription factor MLTF/USF (where MLTF is major late transcription factor). The footprint on the NF-1a site was erroneously identified as MREe in a previous study [16]. Formation of the complex at the level of MREd was inhibited by incubation with excess of the specific MREd oligo, but not by the mutated MUTds competitor (results not shown). These results indicated that other protein species co-purified with MEP-1. Indeed, on an SDS-containing gel, several bands were present (Figure 1B).

In good agreement with the DNaseI footprinting data, EMSA analysis showed that the MRE-binding activity is present in fractions 6–9 of the second affinity column (Figure 1C). Fraction 5, which generated a strong footprint on the NF-1a, NF-1b, USF-a and USF-b sites, did not bind the MRE probe, as assayed by EMSA, thus confirming that the MREd-binding protein is distinct from those binding to these other sites. Notably, the MEP-1–MRE-s complexes migrated faster than those with MTF-1 (Figure 1C; compare lanes 6–9 and COS), thus suggesting that the M_r of MEP-1 is lower than that of MTF-1, and that MEP-1 is distinct from MTF-1.

Western analysis using an anti-MTF-1 polyclonal antibody showed that protein species cross-reacting with the anti-MTF-1 antibody were present in the MEP-1 preparation (results not shown). To test whether MEP-1 and MTF-1 are distinct protein species that could interact with each other and form heterodimeric complexes on MRE DNA, we performed EMSA using MTF-1-enriched COS cell extracts and purified MEP-1 in the same reaction, and the MRE-s oligo as the probe. Figure 2(B) shows

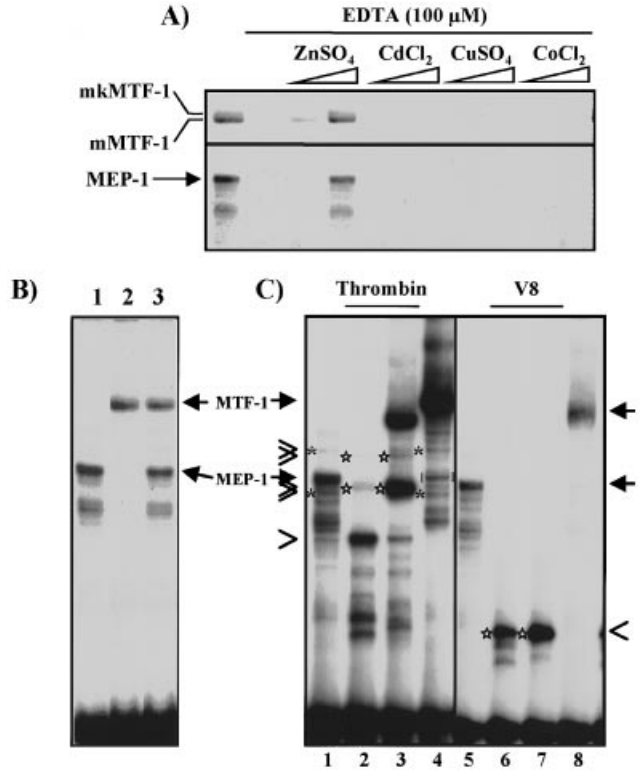

Figure 2 Characterization of MEP-1 and MTF-1

(**A**) Ability of different cations to restore MEP-1 and MTF-1 binding activity on the MRE-s oligo probe following EDTA chelation. Samples of a mouse MTF-1-enriched COS cell nuclear extract or purified MEP-1 were treated for 10 min at 21 °C without or with 100 μM EDTA and then incubated for 10 min at 21 °C in the presence of 5 or 50 μM $ZnSO_4$, $CdCl_2$, $CuSO_4$ or $CoCl_2$, as indicated, and assayed by EMSA. Binding reactions were performed on ice for 10 min. Upper and lower panels are from different gels. MkMTF-1, endogenous monkey (COS cell) MTF-1; mMTF-1, mouse MTF-1. (**B**) EMSA reactions were performed with purified MEP-1 (lane 1), an MTF-1-enriched COS cell extract (lane 2) alone, or with both COS-MTF-1 and MEP-1 in the same EMSA reaction (lane 3). (**C**) Proteolytic EMSA. Binding reactions were performed using the MRE-s probe and purified MEP-1 (lanes 1, 2 and 5, 6) or MTF-1-enriched COS cell nuclear extracts (lanes 3, 4 and 7, 8). COS-cell nuclear extracts and purified MEP-1 were incubated with thrombin (5 min) or staphylococcal proteinase V8 (30 min) at 21 °C, as indicated. Then the labelled MRE-s probe was added to the reaction mixtures, binding was allowed to proceed for 10 min on ice, and samples were analysed by PAGE. The arrowheads indicate the proteinase-resistant specific MRE-s protein complexes. Bands indicated by an arrowhead are also marked with an asterisk or a star and shows co-migrating DNA–protein complexes. The pair of square brackets (lane 4) indicates an MRE-s–protein complex in the COS-cell extract co-migrating with the main MEP-1 complex. The upper right side arrow indicates MTF-1, whereas the lower indicates MEP-1. Autoradiograms were digitally generated as described in the legend to Figure 1.

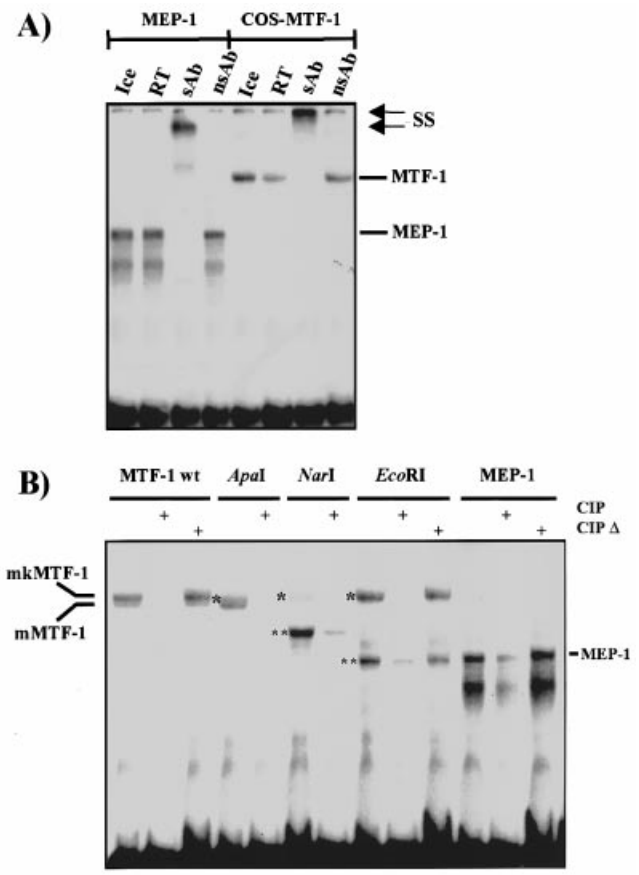

Figure 3 Antibody competition EMSA experiments and deletion mutant analysis

(**A**) EMSA was performed with purified MEP-1 or extracts prepared from COS cells transfected with an MTF-1 expression vector. Anti-MTF-1 antibody (sAb) or non-specific anti-MT-3 antibody (nsAb) was added to the EMSA reaction mixtures, which were preincubated for 5 min at 21 °C before the addition of ^{32}P-labelled MRE-s oligos and an incubation of 10 min on ice. Control reaction mixtures were preincubated with buffer on ice or at 21 °C (RT). SS refers to supershifted complexes. (**B**) EMSA were performed using purified MEP-1, nuclear extracts from COS cells transfected with wild-type MTF-1 or various deletion mutants in which the carboxy region of MTF-1 was deleted from the *Apa*I, the *Nar*I or the *Eco*RI sites, as indicated. A map of MTF-1 is shown in Figure 4B. Note that the complexes generated by the endogenous COS-cell MTF-1 (mkMTF-1, single asterisk) migrate higher on the gel than those produced by the different mouse MTF-1 (mMTF-1, double asterisk) proteins. In some reaction mixtures MEP-1 or COS-cell nuclear extracts were treated with CIP for 5 min at 21 °C before the addition of the probe. The phosphatase-treated samples were then incubated for another 10 min on ice with the probe. Purified MEP-1 and nuclear extracts were also treated with heat-inactivated CIP (CIPΔ) as control. Autoradiograms were digitally generated as described in the legend to Figure 1.

that MEP-1 and MTF-1 gave rise to two distinct migrating bands co-migrating with those obtained when the two proteins are analysed separately, thus showing that MEP-1 does not form a complex with MTF-1. In addition, DNA-binding activity of both protein species is sensitive to EDTA chelation and can be restored by the exogenous addition of $ZnSO_4$ but not by $CdCl_2$, $CuSO_4$ or $CoCl_2$ (Figure 2A).

To define further the relationship between MEP-1 and MTF-1, we used a protease-mediated partial-digestion method coupled with EMSA. Thrombin digestion of MTF-1 and MEP-1 resulted in the formation of numerous MRE complexes, some of them displaying the same mobility shift (Figure 2C; arrowheads). Staphylococcal-V8-proteinase digestion of MTF-1 and MEP-1 resulted in the appearance of a prevalent smaller complex that displayed the same mobility shift (Figure 2C). Furthermore, COS-cell extracts contain a MTF-1–MRE-s complex co-migrating with the main MEP-1–MRE-s complex (Figure 2C, lane 4, square-bracketed). These results suggest that MEP-1–MRE-s complexes contain MTF-1-related proteins. In addition, the fact that neither MEP-1 nor MTF-1 activity was detected in extracts prepared from the MTF-1-null mutant dko7 cells, as assayed by EMSA (results not shown), suggests that MEP-1 and MTF-1 are encoded by the same gene. To further test this hypothesis, the effect of MTF-specific antibody was tested in super-shift experiments. Figure 3(A) shows that anti-MTF-1 antisera

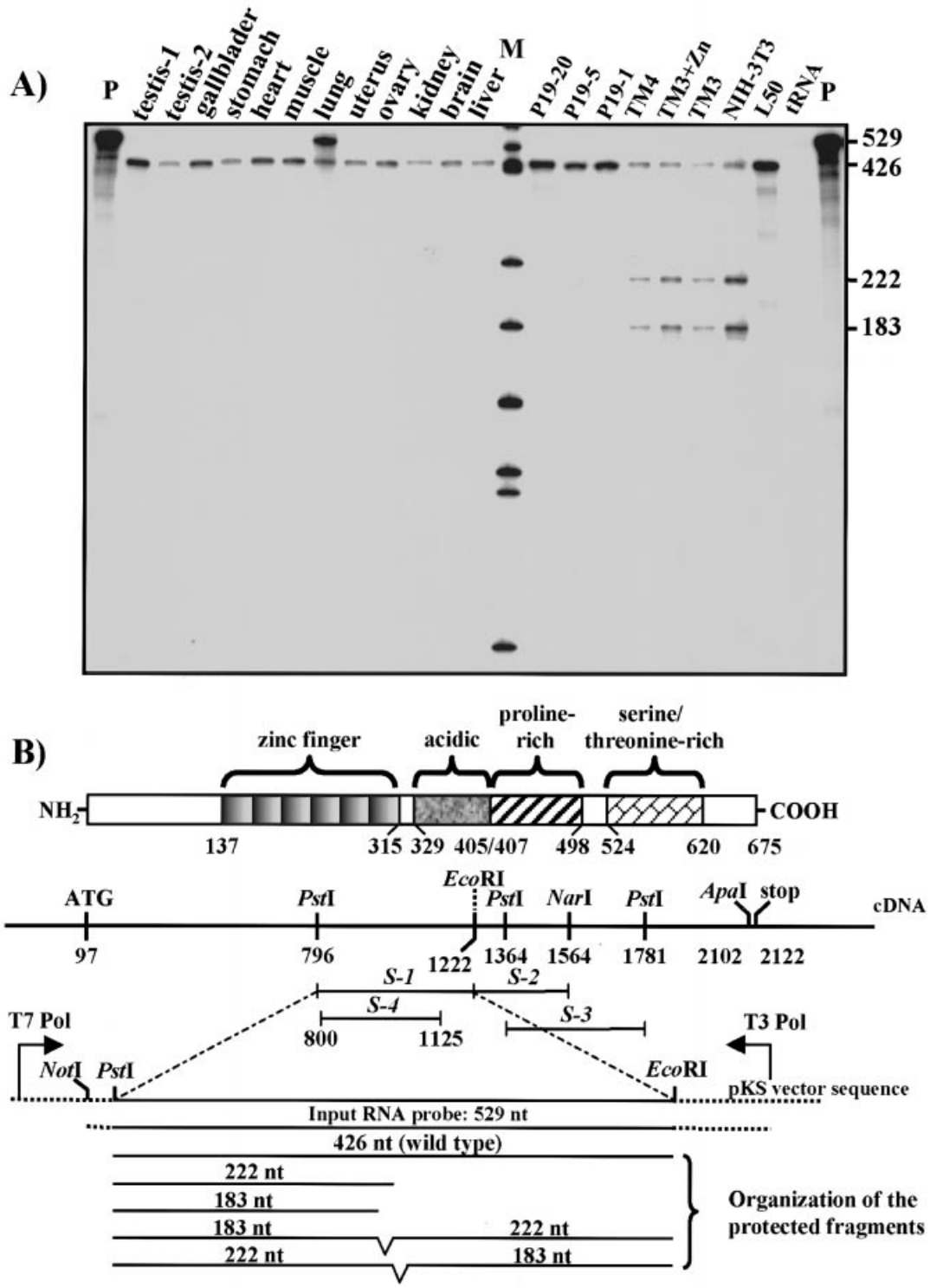

Figure 4 RNase protection analysis

(**A**) Analysis of MTF-1 gene expression in selected tissues and cell lines. An RNase protection assay was carried out with a 529-nucleotide MTF-1 antisense riboprobe (*S-1*) containing sequences from the carboxy region of the Zn-finger domain and most of the acidic domain (**B**). A 20 μg portion of total RNA was incubated with ^{32}P-labelled antisense riboprobe for each sample, except for testes, for which 1 μg (testis-1) and 2 μg (testis-2) were used. RNase-protected RNA fragments were analysed using 6% polyacrylamide/8 M urea gels and autoradiography. Approx. 1.0×10^3 c.p.m. of undigested probe was loaded (lanes P). Yeast tRNA (tRNA) was used as a negative control. The expected protected fragment of 426-nucleotide corresponding to wild-type RNA was detected in all samples, while mRNA isolated from TM3, TM4 and NIH-3T3 cells also protects two regions of 183 and 222 nucleotides, suggesting the existence of alternative splicing, as indicated in (**B**). In lung RNA, a fraction of the MTF-1 riboprobe (indicated as 529) was not fully digested by the ribonuclease treatment. Size markers (M) are *Msp*I digests of pKS DNA, end-labelled with T4 polynucleotide kinase. Numbers on the right indicate the length of the protected fragments in nucleotides. (**B**) Schematic representation of the mouse MTF-1 protein and cDNA with a partial restriction map. *S-1*–*S-4* indicate the different restriction fragments from the mouse MTF-1 cDNA clone cloned downstream of the T3 or T7 RNA polymerase promoter and used to produce synthetic RNA fragments for RNase protection assays. The lower section of the Figure shows the organization of the protected fragments consistent with the results of the assay shown in (**A**). Autoradiograms were digitally generated as described in the legend to Figure 1.

treatment of the MTF-1-enriched COS cell extract or purified MEP-1 eliminated both MTF-1 and MEP-1 mobility complexes and generated a supershift (see also Figure 6 below), whereas anti-MT-3 antibody affected neither the MEP-1–MRE nor the MTF-1–MRE complexes. These results clearly show that MEP-1 is antigenetically related to MTF-1. EMSA experiments performed with various MTF-1 deletion mutants indicate that MEP-1 may correspond to an MTF-1 fragment truncated at a position located between the *Eco*RI (position 1221) and the *Nar*I (position 1564) sites, since the corresponding mutant proteins generated complexes migrating with an electrophoretic mobility close to that of those formed with MEP-1 (Figure 3B). In the mobility-shift assays showing MEP-1 binding (Figures 1C, 2 and 3) there are usually secondary lower-molecular-mass complexes. These complexes most likely represent short MTF-1 fragments, since the anti-MTF-1 antibody can supershift them [Figures 3A, and Figure 6 (below)]. In fact, MEP-1 may correspond to a MTF-1 proteolytic fragment or a MTF-1 splicing variant.

Ribonuclease protection analysis

To determine whether MEP-1 corresponds to a MTF-1 splicing variant, RNase protection experiments were performed using RNA preparations from various tissues and cell lines. Since a MTF-1 clone truncated at the *Eco*RI site generated a protein forming a MRE complex migrating to a position close to that obtained with purified MEP-1 (Figure 3B), we reasoned that a putative MTF-1 splicing variant with a 3′ end located close to this site could exist in the cell. Thus the different probes (*S-1*–*S-4*; Figure 4B) utilized in the present study cover the region around this *Eco*RI site. RNase protection with probe *S-1* (nucleotides 796–1222) identified a transcript corresponding to the wild-type MTF-1 transcript with the expected length of 426 nucleotides in all tissues and cell lines examined (Figure 4A). In addition, in control NIH-3T3, TM3 and TM4, and in Zn^{2+}-treated TM3 cells, two other fragments of 222 and 183 nucleotides were protected (Figure 4A), thus suggesting the existence of MTF-1 splicing variants. The two shorter fragments correspond to putative transcripts with a 3′ end mapping at nucleotides 979 and 1018 in the sixth Zn-finger respectively. Such transcripts would encode proteins with an M_r consistent with that deduced for MEP-1. These fragments could also correspond to transcripts with a short internal deletion in the sixth Zn-finger, as schematically represented in Figure 4(B). However, the putative proteins encoded by such variants would produce MRE complexes migrating with properties similar to those generated by MTF-1, and would have gone undetected in EMSA. To discriminate between these two possibilities, RNase protection analyses were performed using probe *S-4*. Using this probe, three fragments of 325, 180 and 125 nucleotides of similar intensity were protected, consistent with the existence of a splicing variant containing an internal deletion of 21 nucleotides (positions 979 to 1000) in the sixth Zn-finger (results not shown). However, a problem occasionally encountered with the RNase protection assay is the internal cleavage of RNA duplexes during RNase digestion. This leads to a loss of the full-length protected product and the generation of small subfragments. This problem is solved by omitting RNase A from the digestions [23]. In fact, the 180- and 125-nucleotide fragments were not detected with probe *S-4* if RNase A was omitted from the reaction (results not shown), thus indicating that they do not correspond to *bona fide* transcripts and are generated by the RNase A enzyme. Moreover increasing the amount of RNase A in the assay led to the complete elimination of the 426-nucleotide transcript for the 222- and 183- nucleotide fragments (results not shown). To confirm that there is no differential splicing occurring in this region of the MTF-1 gene, MTF-1 transcripts were amplified by RT-PCR, using as the template total RNA from NIH-3T3. DNA sequence analyses performed on six clones obtained from two different RT-PCR reactions failed to reveal the existence of any spliced variant RNA (results not shown). Using probes *S-2* and *S*-3, a single protected fragment corresponding to MTF-1 wild-type RNA was detected (results not shown). Overall these results show that no splicing variant corresponding to MEP-1 could be identified in any cell lines or tissues analysed in the present study. These RNase protection analyses also showed that MTF-1 is expressed at constant low levels in all tissues and cell lines examined, except in the testes, where, as reported previously [11,27], MTF-1 mRNA levels were approx. 10-fold higher than those present in other tissues. The physiological meaning of high MTF-1 mRNA levels in the testes remains unclear.

Analysis of MTF-1 DNA-binding activity

MTF-1 appears to be reversibly activated to bind to DNA and enhance MT gene transcription in response to increased Zn^{2+} levels [5,28–30]. Indeed, MTF-1 binding in nuclear extracts from Zn^{2+}-pretreated cells was 3–8-fold higher than that in nuclear extracts from untreated cells (Figures 5A, 5B, 5C, 5D and 5F). Increased MTF-1 binding activity is very rapid and reaches its maximum as soon as 20 min after Zn^{2+} treatment of cultured cells (Figure 5B). However, MTF-1 binding activity in extracts prepared from cells treated with $CdCl_2$ (30 min–8 h), PMA (8 h) or UV irradiation (100 J/m^2) were similar to that measured in control cells (Figures 5A and 5B), despite strong induction of MT gene transcription as assayed by Northern analysis (results not shown).

Other studies have indicated that MTF-1 in extracts from control Hepa cells can be activated *in vitro* by the addition of Zn^{2+} followed by incubation at 37 °C [29,31]. In the present study, DNA binding of MTF-1 to the probe occurs as efficiently on ice as at 21 °C, and the addition of exogenous Zn^{2+} to EMSA reactions performed with control or Zn^{2+}-treated cell extracts, or preincubation of EMSA reaction mixtures at 37 °C, did not increase MTF-1 binding activity (Figures 5C and 5D). In fact, DNA binding was markedly inhibited when the extract was preincubated at 37 °C. As reported by Dalton et al. [29], the addition of exogenous Zn^{2+} (30 μM) during the 37 °C incubation period efficiently protected MTF-1 from being inhibited (Figure 5D). Similarly, DNA-binding activity of recombinant mouse MTF-1 synthesized in a reticulocyte lysate is dependent on the addition of exogenous Zn^{2+} to the binding reaction (Figure 5E) [29,31] and occurred on ice, at 21 °C and at 37 °C, although it was optimal at 21 °C.

Notably, in control cell extracts, approx. 16% of MTF-1 binding activity is detected in the cytosol and 84% in nucleus, whereas in extracts prepared from Zn^{2+}-treated cells almost 100% of the activity was present in the nuclear fraction (Figure 5F). Control experiments using an Sp1 binding site in the EMSA showed that the cytosol extracts were completely devoid of Sp1 activity (Figure 5F), thus showing that they were not significantly contaminated with nuclear proteins. To determine whether MTF-1 in the cytosolic fraction can be activated *in vitro*, Zn^{2+} (30 μM) was added to the extract and incubated at 37 °C for 15 min. Then the MRE-s probe was added and incubation was continued for 10 min at 21 °C or on ice. However, this procedure

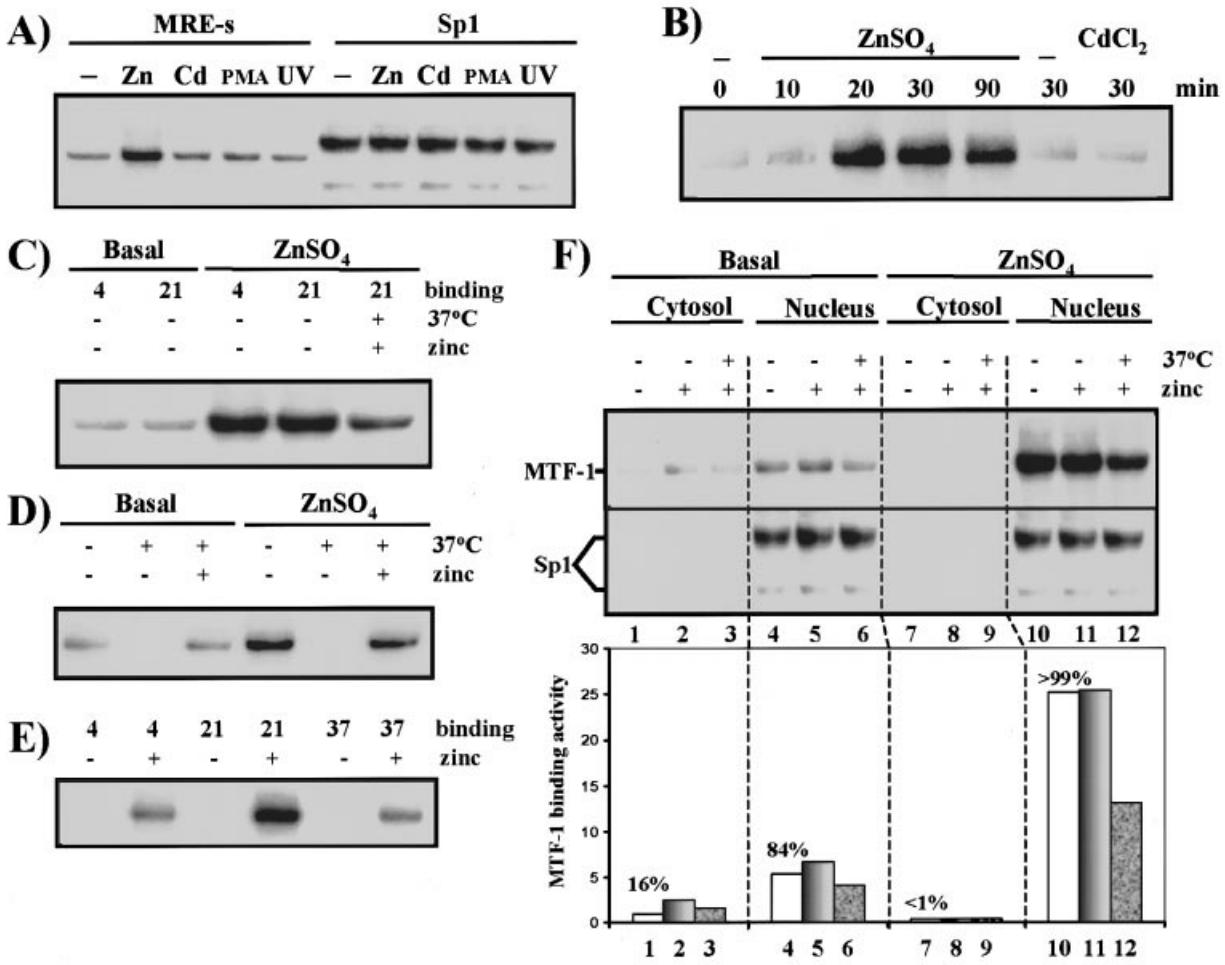

Figure 5 Activation of MTF-1 DNA-binding activity

(**A**) Mouse L50 cells were incubated for 30 min in medium containing 100 μM $ZnSO_4$, 2.5 μM $CdCl_2$, or 8 h in the presence of 100 ng/ml PMA, or irradiated with a UV germicidal lamp (254 nm, 100 J/m^2) and harvested 8 h later. Aliquots of nuclear extracts (2 μg) were analysed by EMSA using labelled MRE-s or Sp1 oligos, as indicated. Binding reaction mixtures were incubated on ice for 10 min and subjected to PAGE. Gels were dried, and labelled MRE-s was detected by autoradiography. Only those regions of the gels containing the specific MTF-1 or Sp1 complexes are shown. –, No treatment. (**B**) L50 cells were incubated for the indicated time in medium containing 100 μM $ZnSO_4$ or 2.5 μM $CdCl_2$ and EMSA was performed as described in (**A**). –, No treatment. (**C**) Nuclear extracts were prepared from control (Basal) or Zn^{2+}-treated ($ZnSO_4$; 30 min, 100 μM) L cells and analysed by EMSA using the MRE-s probe. Binding reactions (binding) were performed on ice (4) or 21 °C (21) for 10 min, preceded or not by a preincubation of 15 min at 37 °C in the presence of 30 μM $ZnCl_2$ (zinc), as indicated. (**D**) Control (Basal) or Zn^{2+}-treated ($ZnSO_4$) L-cell nuclear extracts were prepared and analysed by EMSA using a labelled MRE-s oligo probe. Where indicated binding reactions were adjusted to the final concentration of 30 μM of exogenous Zn^{2+} (zinc), incubated at 37 °C, or kept on ice, for 15 min, labelled MRE-s was added and the incubation was continued on ice for 10 min. (**E**) Zn^{2+}-dependent activation of recombinant MTF-1 synthesized *in vitro* in a TnT lysate. EMSA was performed using recombinant mouse MTF-1 synthesized *in vitro* in a coupled transcription–translation lysate. Binding-reaction mixtures containing labelled MRE-s oligo and 30 μM $ZnCl_2$ (zinc) were incubated on ice (4) or at 21 °C (21) or 37 °C (37), as indicated. (**F**) EMSA detection of MTF-1 in nuclear and cytosolic extracts from L cells. Upper panel: L cells were treated with 100 μM $ZnSO_4$ for 30 min. Nuclear and cytosolic extracts were prepared from treated or untreated cells and analysed for DNA-binding activity using a labelled MRE-s or Sp1 oligo. Where indicated, binding reactions were adjusted to the final concentration of 30 μM of exogenous Zn^{2+} (zinc), incubated at 37 °C, or kept on ice, for 15 min, labelled MRE-s was added and the incubation was continued on ice for 10 min. Bottom panel: graphic representation of MTF-1 DNA-binding activity obtained with the EMSA shown in the upper panel. The amount of MTF-1-MRE-s binding complex was quantified by PhosphoImager analysis. Percentages indicate the amount of MTF-1 DNA-binding activity detected in cytosol and nucleus in control and Zn^{2+}-treated cells. All data are representative of at least three separate experiments. Autoradiograms were digitally generated as described in the legend to Figure 1.

did not increase MTF-1 DNA-binding activity in the cytosolic extract (Figure 5F).

Role of phosphorylation in the activation of MTF-1

To assess the possible role of phosphorylation in the activation of MTF-1 DNA-binding activity, MTF-1-enriched COS-cell nuclear extracts and purified MEP-1 were treated with CIP and analysed by EMSA. In parallel, nuclear extracts were treated with heat-inactivated phosphatase as controls. Treatments with CIP almost completely abrogated MTF-1–MRE complex-formation in nuclear extracts from control (results not shown) and Zn^{2+}-treated cells (Figures 3B and 6), whereas those with MEP-1 were not as much affected. By contrast, heat-inactivated phosphatase had no effect on MTF-1 binding activity. Similarly the MTF-1-*Nar*I and MTF1-*Eco*RI mutants are also partially resistant to CIP inactivation (Figure 3B). These findings indicate that phosphorylation is involved in the regulation of MTF-1 activity. These results also show that removal of the C-terminal region of MTF-1, as in MEP-1, renders the mutant protein partially resistant to the inhibitory effects of phosphatases.

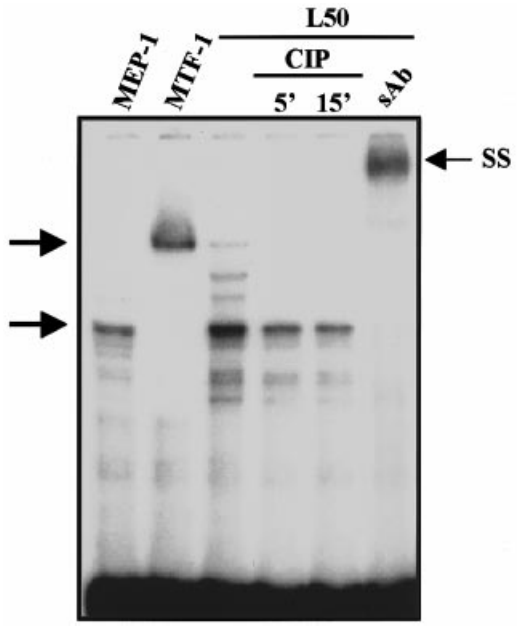

Figure 6 Effects of phosphatase treatment on MEP-1 and MTF-1 DNA-binding activities

L50-cell nuclear extracts (2 μg) were treated with CIP for 5 or 15 min at 21 °C, as indicated. Nuclear extracts were also treated with heat-inactivated CIP as control (Figure 3B and results not shown). The treated nuclear extracts were incubated with ^{32}P-labelled MRE-s oligo and analysed by EMSA. Where indicated, anti-MTF-1 antibody (sAb) was added to the binding reaction mixture as described in Figure 3(B). EMSA reactions were also performed with purified MEP-1 (MEP-1) and MTF-1-enriched COS-cell nuclear extracts (MTF-1), as indicated. The upper arrow indicates MTF-1 and the lower MEP-1. Note that the L50-cell extract contains MEP-1 and MTF-1 DNA-binding activities and that the anti-MTF-1 antibody eliminated both MTF-1 and MEP-1 mobility complexes and generated a supershift. SS refers to supershifted complexes. Autoradiograms were digitally generated as described in the legend to Figure 1.

DISCUSSION

MTF-1 is essential for basal and metal-induced MT gene transcription and appears to be the only factor that binds MREs, and the only transcription factor that mediates responsiveness to different metals [6,11]. However, we previously identified and characterized a nuclear protein termed MEP-1 that binds the MREs of the mouse MT-1 gene in a Zn^{2+}-dependent manner [15,16]. Here we examined the relationship between MEP-1 and MTF-1, and showed that MEP-1 is antigenically related to MTF-1. RNase protection experiments failed to reveal the presence of any MTF-1 splicing variants corresponding to MEP-1 (Figure 4). This is in agreement with Brugnera et al. [32], who did not find evidence for alternative splicing or an MTF-1 gene family. Thus MEP-1 appears to correspond to an MTF-1 proteolytic fragment. Since MEP-1 is recognized by an anti-MTF-1 antibody raised against a synthetic peptide derived from the N-terminal region [7], we assume that MEP-1 is missing approx. 300 residues of the C-terminal region. This corresponds to a cleaving point located close to the *Eco*RI site and, in fact, MTF-1-*Eco*RI mutant-MRE-s complexes migrate to a position very near to those made with MEP-1 (Figure 3B). Thus our results further support the contention that MTF-1 is the major, if not the only, MRE-binding factor.

It has been suggested that MTF-1 functions as a reversible activated sensor of free Zn^{2+} pool in the cell, and is reversibly activated to bind to DNA in response to increased free Zn^{2+} levels [5,28–30]. Notably, nuclear MTF-1 activity rapidly increased between 3- and 10-fold more within 20 min of treatment with Zn^{2+} (Figures 5A–5D and 5F). However, untreated control cells appear to contain active MTF-1 molecules, since MTF-1 DNA binding was detected in control cell nuclear extracts, as assayed by EMSA (Figure 5). It is possible that, in the non-induced state, Zn^{2+} ions present in the cell allow some MTF-1 molecules to exist in an active DNA-binding form. Extracts prepared from control cells presumably contain enough endogenous Zn^{2+} to keep some of the protein–DNA complexes together, even though the nuclear extract is diluted 12-fold in the EMSA binding reactions. Increases in intracellular Zn^{2+} concentrations would augment the pool of active molecules and thereby increase the MT gene transcription rate. Three lines of evidence support this hypothesis: first, *in vivo* footprinting experiments revealed that detectable protection was dependent on Zn^{2+} induction at all MRE except MREd, where metal treatment enhances a pre-existing low-level protection [33]. Thus the strongest MRE in the mouse MT-1 gene promoter shows a detectable footprint in the absence of added metal; secondly, in MTF-1 null mutant cells, the endogenous MT genes are silent both before and after treatment of the cells with metals, thus indicating that MTF-1 is important for basal MT gene expression; thirdly, MTF-1 binding activity is readily detectable in control cell extracts (Figures 5A–5D and 5F).

The addition of exogenous Zn^{2+} to EMSA binding reactions or preincubation of control and Zn^{2+}-treated cell extracts at 37 °C did not enhance MTF-1 DNA-binding activity (Figures 5C and 5F). However, others have reported that MTF-1 binding activity could be increased *in vitro* by the addition of Zn^{2+} to control-cell extracts or by a preincubation at 37 °C [6,29,31]. The reason for these apparent discrepancies is not clear, but may reflect differences in the experimental conditions in which EMSA analyses are performed. Zn^{2+} is required for MTF-1 binding activity *in vitro* and EDTA inhibits its binding activity (Figure 2A) [5,6,13,28,29]. EDTA is commonly included during electrophoresis. Gel systems used in the presence of EDTA would be expected to promote dissociation of the MTF-1 complexes, and this might explain reports of low or non-existent MTF-1 binding activity in control-cell extracts, which can be activated *in vitro* in a DNA-binding form.

Regulation of MTF-1 DNA-binding activity was also examined in nuclear and cytosol extracts in response to metal ions. We showed that cytosol extracts prepared from untreated control cells contain 16% of the total MTF-1 DNA-binding activity, whereas the nuclear fraction contained 84%. Furthermore, MTF-1 binding activity decreased to almost undetectable levels in the cytosol of Zn^{2+}-treated cells (Figure 5F), thus confirming the report showing that Zn^{2+} promotes rapid nuclear translocation of MTF-1 [34]. Cytosolic MTF-1 binding activity is clearly not caused by leakage from the nuclei, since the cytosol extracts were completely devoid of Sp1 activity (Figure 5F). Interestingly, in control Hepa cells, only 17% of the immunoreactive MTF-1 was detected in the nuclear fraction, whereas 83% was in the cytosolic fraction [34]. Attempts to activate MTF-1 in the cytosol fraction by the addition of Zn^{2+} followed by incubation at 37 °C did not increase MTF-1 DNA-binding activity (Figure 5F). This indicates that most of the MTF-1 molecules in the cytosol of control cells is in an inactive non-DNA-binding conformation and that, following metal induction, cytosolic MTF-1 is activated and translocated to the nucleus.

The role of Zn^{2+} in MTF-1 activation has been the subject of some controversy. It was suggested that direct and reversible

interactions of Zn^{2+} with the Zn-finger domain of MTF-1 regulate its DNA-binding activity [5,6,29]. Zn^{2+} would lead to an allosteric change in MTF-1, causing exposure of Zn-fingers involved in DNA binding. All the other metals capable of inducing MT would do so by displacing Zn^{2+} from the weakly bound pool, and this displaced Zn^{2+} would activate MTF-1 DNA binding [11]. Consequently, Cd^{2+} should lead to an increase in MTF-1 DNA-binding activity as assayed by EMSA. However, Cd^{2+} (Figures 5A and 5B), as well as other transition metals [31] and hypoxia [9], do not significantly enhance MTF-1 DNA-binding activity *in vivo* and *in vitro*, despite strong MTF-1-dependent induction of MT genes. These data suggest that Zn^{2+} and Cd^{2+} may activate MTF-1 by different mechanisms. This also indicates that MTF-1 activity can be modulated by mechanisms independent of the Zn^{2+}-dependent increase in DNA-binding activity and that Zn^{2+}-induction *in vivo* could induce other changes in MTF-1, distinct from the structural changes directly induced by Zn^{2+}.

In addition to the direct interaction of Zn^{2+} with MTF-1, other signal-transduction cascades may be involved in the regulation of MTF-1 activity in response to metal ions or during hypoxia. This can be accomplished by post-translational modifications such as phosphorylation. In fact, we showed that phosphatase treatments strongly abrogate MTF-1 DNA-binding activity (Figures 3 and 6). This suggests that phosphorylation is involved in the regulation of MTF-1 activity. Activation of MT gene transcription in response to ROS is largely mediated by MTF-1 [8], whereas that in response to hypoxia is entirely mediated by MREs and MTF-1 [9]. This indicates that metals are not the only factors regulating MTF-1 activity. ROS and hypoxia have been implicated in the activation of various kinase signalling cascades, including protein kinase C (PKC), mitogen-activated protein kinase and phosphatidylinositol 3-kinase, with changes in downstream effectors such as hypoxia-inducible factor, the protein Elk-1, the proto-oncogene proteins c-Jun and c-Fos, the protein p53 and nuclear factor κB [35–37]. Some of these kinases may be involved in the phosphorylation of MTF-1. In this regard, it is noteworthy that inhibition of PKC by prolonged exposure to phorbol ester blocked Zn^{2+}- and Cd^{2+}-mediated activation of the MRE in HepG2 cells [38]. This suggests that PKC is involved in the process of metal-induced MT gene expression and supports the contention that MTF-1 activity can be regulated by phosphorylation.

We thank Walter D. Schaffner for providing the MTF-1 expression vector and the anti-MTF-1 polyclonal antibody, and Harold Gaboury for his help with the English presentation of this text. O.LaR. was supported by Predoctoral Fellowships from the Fonds pour la Formation des Chercheurs et l'Aide à la Recherche du Québec and the Conseil de recherches en sciences naturelles et en génie du Canada (CRSNG), and P.M. by a Postdoctoral Fellowship of the Fédération québécoise des sociétés Alzheimer, and the Société Alzheimer du Canada. This research was supported by a grant from the CRSNG to C.S.

REFERENCES

1 Moffatt, P. and Denizeau, F. (1997) Metallothionein in physiological and physiopathological processes. Drug Metab. Rev. **29**, 261–307
2 Palmiter, R. D. (1998) The elusive function of metallothioneins. Proc. Natl. Acad. Sci. U.S.A. **95**, 8428–8430
3 Carter, A. D., Felber, B. K., Walling, M. J., Jubier, M. F., Schmidt, C. J. and Hamer, D. H. (1984) Duplicated heavy metal control sequences of the mouse metallothionein-I gene. Proc. Natl. Acad. Sci. U.S.A. **81**, 7392–7396
4 Stuart, G. W., Searle, P. F., Chen, H. Y., Brinster, R. L. and Palmiter, R. D. (1984) A 12-base-pair DNA motif that is repeated several times in metallothionein gene promoters confers metal regulation to a heterologous gene. Proc. Natl. Acad. Sci. U.S.A. **81**, 7318–7322
5 Radtke, F., Heuchel, R., Georgiev, O., Hergersberg, M., Gariglio, M., Dembic, Z. and Schaffner, W. (1993) Cloned transcription factor MTF-1 activates the mouse metallothionein-I promoter. EMBO J. **12**, 1355–1362
6 Heuchel, R., Radtke, F., Georgiev, O., Stark, G., Aguet, M. and Schaffner, W. (1994) The transcription factor MTF-1 is essential for basal and heavy metal-induced metallothionein gene expression. EMBO J. **13**, 2870–2875
7 Radtke, F., Georgiev, O., Muller, H. P., Brugnera, E. and Schaffner, W. (1995) Functional domains of the heavy metal-responsive transcription regulator MTF-1. Nucleic Acids Res. **23**, 2277–2286
8 Dalton, T. P., Li, Q., Bittel, D., Liang, L. and Andrews, G. K. (1996) Oxidative stress activates metal-responsive transcription factor-1 binding activity. J. Biol. Chem. **271**, 26233–26241
9 Murphy, B. J., Andrews, G. K., Bittel, D., Discher, D. J., McCue, J., Green, C. J., Yanovsky, M., Giaccia, A., Sutherland, R. M., Laderoute, K. R. and Webster, K. A. (1999) Activation of metallothionein gene expression by hypoxia involves metal response elements and metal transcription factor-1. Cancer Res. **59**, 1315–1322
10 Maur, A. A. D., Belser, T., Elgar, G., Georgiev, O. and Schaffner, W. (1999) Characterization of the transcription factor MTF-1 from the Japanese pufferfish (*Fugu rubripes*) reveals evolutionary conservation of heavy metal stress response. Biol. Chem. **380**, 175–185
11 Palmiter, R. D. (1994) Regulation of metallothionein genes by heavy metals appears to be mediated by a zinc-sensitive inhibitor that interacts with a constitutively active transcription factor, MTF-1. Proc. Natl. Acad. Sci. U.S.A. **91**, 1219–1223
12 Labbé, S., Simard, C. and Séguin, C. (1997) Metallothionein gene regulation in mouse cells. In Metal Ions in Gene Regulation (Silver, S. and Walden, W., eds.), pp. 231–249, Chapman and Hall, New York
13 Otsuka, F., Iwamatsu, A., Suzuki, K., Ohsawa, M., Hamer, D. H. and Koizumi, S. (1994) Purification and characterization of a protein that binds to metal responsive elements of the human metallothionein II(A) gene. J. Biol. Chem. **269**, 23700–23707
14 Remondelli, P. and Leone, A. (1997) Interactions of the zinc regulated factor (ZiRF1) with the mouse metallothionein Ia promoter. Biochem. J. **323**, 79–85
15 Labbé, S., Prévost, J., Remondelli, P., Leone, A. and Séguin, C. (1991) A nuclear factor binds to the metal regulatory elements of the mouse gene encoding metallothionein-I. Nucleic Acids Res. **19**, 4225–4231
16 Labbé, S., Larouche, L., Mailhot, D. and Séguin, C. (1993) Purification of mouse MEP-1, a nuclear protein that binds to the metal regulatory elements of genes encoding metallothionein. Nucleic Acids Res. **21**, 1549–1554
17 Rudnicki, M. A. and McBurney, M. W. (1987) Cell culture methods and induction of differentiation of embryonal carcinoma cell lines. In Teratocarcinomas and Embryonic Stem Cells: A Practical Approach (Robertson, E. J., ed.), pp. 19–49, IRL Press, Oxford
18 Sambrook, J., Fritsch, E. F. and Maniatis, T. (1989) Molecular Cloning: A Laboratory Manual, Cold Spring Harbor Laboratory Press, Cold Spring Harbor, NY
19 Séguin, C. and Hamer, D. H. (1987) Regulation *in vitro* of metallothionein gene binding factors. Science **235**, 1383–1387
20 Schreiber, E., Matthias, P., Müller, M. M. and Schaffner, W. (1989) Rapid detection of octamer binding proteins with "mini-extracts", prepared from small number of cells. Nucleic Acids Res. **17**, 6419
21 Séguin, C. and Prévost, J. (1988) Detection of a nuclear protein that interacts with a metal regulatory element of the mouse metallothionein 1 gene. Nucleic Acids Res. **16**, 10547–10560
22 Kingston R. E., Chomczynski P. and Sacchi N. (1995) Guanidine methods for total RNA preparation. In Current Protocols in Molecular Biology (Ausubel F. M., Brent, R., Kingston R. E., Moore D. D., Seidman J. G., Smith J. A. and Struhl K., eds.), pp. 4.2.1–4.2.9, Greene Publishing Associates and Wiley Interscience, New York
23 Gilman M. (1993) Ribonuclease protection assay. In Current Protocols in Molecular Biology (Ausubel F. A., Brent R., Kingston R. E., Moore D. D., Seidman J. G., Smith, J. A. and Struhl K., eds.), pp. 4.7.1–4.7.8, Greene Publishing Associates and Wiley Interscience, New York
24 Bordonaro, M., Saccomanno, C. F. and Nordstrom, J. L. (1994) An improved T1/A ribonuclease protection assay. Biotechniques **16**, 428–430
25 Sanger, F., Nicklen, S. and Coulson, A. R. (1977) DNA sequencing with chain terminating inhibitors. Proc. Natl. Acad. Sci. U.S.A. **74**, 5463–5467
26 Del Sal, G., Manfioletti, G. and Schneider, C. (1989) The CTAB-DNA precipitation method: A common mini-scale preparation of template DNA from phagemids, phages or plasmids suitable for sequencing. Biotechniques **7**, 514–520
27 Moffatt, P. and Séguin, C. (1998) Expression of the gene encoding metallothionein-3 in the organs of the reproductive system. DNA Cell Biol. **17**, 501–510
28 Westin, G. and Schaffner, W. (1988) A zinc-responsive factor interacts with a metal-regulated enhancer element (MRE) of the mouse metallothionein-I gene. EMBO J. **7**, 3763–3770
29 Dalton, T. P., Bittel, D. and Andrews, G. K. (1997) Reversible activation of mouse metal response element-binding transcription factor 1 DNA binding involves zinc interaction with the zinc finger domain. Mol. Cell Biol. **17**, 2781–2789

30 Koizumi, S., Suzuki, K., Ogra, Y., Yamada, H. and Otsuka, F. (1999) Transcriptional activity and regulatory protein binding of metal-responsive elements of the human metallothionein-IIA gene. Eur. J. Biochem. **259**, 635–642
31 Bittel, D., Dalton, T., Samson, S. L. A., Gedamu, L. and Andrews, G. K. (1998) The DNA binding activity of metal response element-binding transcription factor-1 is activated *in vivo* and *in vitro* by zinc, but not by other transition metals. J. Biol. Chem. **173**, 7127–7133
32 Brugnera, E., Georgiev, O., Radtke, F., Heuchel, R., Baker, E., Sutherland, G. R. and Schaffner, W. (1994) Cloning, chromosomal mapping and characterization of the human metal-regulatory transcription factor MTF-1. Nucleic Acids Res. **22**, 3167–3173
33 Mueller, P. R., Salser, S. J. and Wold, B. (1988) Constitutive and metal-inducible protein : DNA interactions at the mouse metallothionein I promoter examined by *in vivo* and *in vitro* footprinting. Genes Dev. **2**, 412–427
34 Smirnova, I. V., Bittel, D. C., Ravindra, R., Jiang, H. and Andrews, G. K. (2000) Zinc and cadmium can promote rapid nuclear translocation of metal response element-binding transcription factor-1. J. Biol. Chem. **275**, 9377–9384
35 Adler, V., Yin, Z. M., Tew, K. D. and Ronai, Z. (1999) Role of redox potential and reactive oxygen species in stress signaling. Oncogene **18**, 6104–6111
36 Royds, J. A., Dower, S. K., Qwarnstrom, E. E. and Lewis, C. E. (1998) Response of tumour cells to hypoxia : role of p53 and NF-κB. Mol. Pathol. **51**, 55–61
37 Richard, D. E., Berra, E., Gothie, E., Roux, D. and Pouysségur, J. (1999) p42/p44 mitogen-activated protein kinases phosphorylate hypoxia-inducible factor 1α (HIF-1α) and enhance the transcriptional activity of HIF-1. J. Biol. Chem. **274**, 32631–32637
38 Chu, W. A., Moehlenkamp, J. D., Bittel, D., Andrews, G. K. and Johnson, J. A. (1999) Cadmium-mediated activation of the metal response element in human neuroblastoma cells lacking functional metal response element-binding transcription factor-1. J. Biol. Chem. **274**, 5279–5284

Received 17 August 2000/16 October 2000; accepted 8 November 2000